Theory of noncollinear interactions beyond Heisenberg exchange: Applications to bcc Fe

A. Szilva,[1] D. Thonig,[1] P. F. Bessarab,[2,3] Y. O. Kvashnin,[1] D. C. M. Rodrigues,[1,4] R. Cardias,[1,4] M. Pereiro,[1] L. Nordström,[1] A. Bergman,[5,6] A. B. Klautau,[4] and O. Eriksson[1,7]

[1]*Department of Physics and Astronomy, Division of Materials Theory, Uppsala University, Box 516, SE-75120 Uppsala, Sweden*

[2]*Science Institute of the University of Iceland, 107 Reykjavik, Iceland*

[3]*Department of Nanophotonics and Metamaterials, ITMO University, 197101 St. Petersburg, Russia*

[4]*Faculdade de Física, Universidade Federal do Pará, Belém, 66075-110, Brazil*

[5]*Maison de la Simulation, USR 3441, CEA-CNRS-INRIA-Université Paris-Sud-Université de Versailles, F-91191 Gif-sur-Yvette, France*

[6]*INAC-MEM, CEA, F-38000 Grenoble, France*

[7]*School of Science and Technology, Örebro University, SE-701 82 Örebro, Sweden*

(Received 21 June 2017; revised manuscript received 12 September 2017; published 10 October 2017)

We show for a simple noncollinear configuration of the atomistic spins (in particular, where one spin is rotated by a finite angle in a ferromagnetic background) that the pairwise energy variation computed in terms of multiple-scattering formalism cannot be fully mapped onto a bilinear Heisenberg spin model even in the absence of spin-orbit coupling. The non-Heisenberg terms induced by the spin-polarized host appear in leading orders in the expansion of the infinitesimal angle variations. However, an E_g-T_{2g} symmetry analysis based on the orbital decomposition of the exchange parameters in bcc Fe leads to the conclusion that the nearest-neighbor exchange parameters related to the T_{2g} orbitals are *essentially* Heisenberg-like: they do not depend on the spin configuration, *and* can, in this case, be mapped onto a Heisenberg spin model even in extreme noncollinear cases.

DOI: 10.1103/PhysRevB.96.144413

I. INTRODUCTION

The microscopic origin of the exchange interactions in ferromagnetic bcc Fe (as well as in metallic magnets in general) is part of ongoing scientific discussions [1–3], in spite of the fact that iron is probably the best-known magnet. Especially at finite temperature when the atomistic spin moments deviate from a collinear and uniform direction, i.e., a global magnetization axis cannot be easily identified, the dependence of the interatomic exchange parameters on the underlying spin configuration could become more significant [3]. The lack of a global quantization axis requires the use of a noncollinear framework for calculation of the exchange parameters which are crucial for the interpretation of the experimental observations [4,5]. Based on the classical Heisenberg model,

$$\mathcal{H} = -\sum_{i \neq j} J_{ij} \vec{e}_i \cdot \vec{e}_j \ , \tag{1}$$

where $\vec{e}_i$ ($\vec{e}_j$) is a unit vector pointing in the direction of the atomic moment at site i (j) and J_{ij} stands for the exchange coupling parameter between the magnetic moments, the critical temperature and the magnon excitation spectra of iron at low temperatures can be well described by *ab initio* calculations [3,5–12]. Note that the sum in Eq. (1) avoids double counting.

Although a formula for the exchange coupling J_{ij} in the case of the collinear arrangement has been known for a long time, due to the seminal work of Lichtenstein, Katsnelson, Antropov, and Gubanov (LKAG) [13], even for relativistic [14] and correlated systems [15], a counterpart mapping onto a spin Hamiltonian for the noncollinear arrangement [16] is nontrivial. Similar to the LKAG derivation, a derivation was found in Ref. [17] for the pairwise energy variation based on the magnetic force theorem [18,19] by allowing the presence of a noncollinear underlying spin configuration. The pairwise energy variation term $\delta E_{ij}^{\text{two}}$ emerges for the case when two atomistic spins are infinitesimally rotated at two different sites *at the same time*, and its further analysis is in the scope of this paper. Note that the total energy variation can be written as $\delta E_{ij} = \delta E_i^{\text{one}} + \delta E_j^{\text{one}} + \delta E_{ij}^{\text{two}}$, where the one-site energy variation δE_i^{one} (δE_j^{one}) takes into account the interaction between the spin at site i (j) and the environment formed by the other spins (except for the spins sitting at sites i and j). A system is in equilibrium when δE_i^{one} does not have a finite contribution of leading order in the infinitesimal rotation angle $\delta\theta_i$, when no torques occur within the magnetic state. Note that one can still find noncollinear systems also in equilibrium as the flat spin spirals [20]. By using the noncollinear approach for bcc Fe as well as for Fe overlayers on Ir(001), the magnon softening observed at room temperature in neutron scattering experiments [21] was explained [17,22]. In this paper, we show that in a general, nonequilibrium, noncollinear case, an anisotropic-type term is found that cannot be mapped onto a Heisenberg model given by Eq. (1) even in the absence of spin-orbit coupling. We show, however, that an E_g-T_{2g} symmetry analysis based on the orbital decomposition of J_{ij} leads to a conclusion for the origin of Heisenberg and non-Heisenberg terms similar to what was published in Ref. [2] within the LKAG approach.

Higher-order exchange interactions are known to emerge in the absence of spin-orbit coupling. Recently, the microscopic theory of the magnetic interactions including four-spin exchange was successfully applied to simulate the magnetic phase diagram of heavy rare-earth elements [23]. In the case of bcc Fe, higher-order (biquadratic) exchange interactions also have to be taken into account in the spin Hamiltonian [24–27]. It can be shown that the noncollinear pairwise energy variation formula recovers the pairwise energy formula published in Ref. [24] for a collinear case by keeping the higher- (fourth-) order terms in the infinitesimal angle variation; that is, an anisotropic term is present even in the collinear limit, which was found to be numerically significant in bcc Fe [17].

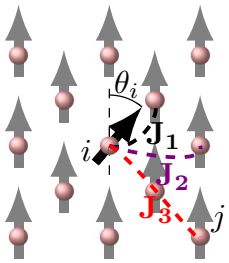

FIG. 1. Schematic representation of the geometry of the *single-spin-rotation system*. As a new system of reference for the infinitesimal two-site spin rotations, an atomistic spin is rotated by a finite θ_i angle at site i on a lattice when every other spin forms a ferromagnetic background. The exchange parameters J_i ($i = 1,2,3,\ldots$) are calculated between the rotated spin at site i and a spin in the ferromagnetic host at site j.

In this paper, we analyze the pairwise energy variation for the system of *single-spin rotation* shown in Fig. 1. The single-spin-rotation problem is a kind of nonequilibrium and noncollinear state in which an atomistic spin is rotated by a finite θ_i angle at site i on a bcc Fe lattice when every other spin forms a collinear ferromagnetic background. It serves here primarily as a good example of how exchange interactions of ferromagnetic materials become modified when the system is brought out of equilibrium. We show that one can find contributing terms in the noncollinear $\delta E_{ij}^{\text{two}}$ that are *essentially* non-Heisenberg of *the leading* (second) order in the infinitesimal angle variation: terms can be found that cannot be mapped onto Eq. (1). This is a different case than a Heisenberg model with spin-configuration-dependent J_{ij}, as defined in Ref. [2], where J_{ij} in Eq. (1) was referred to as the non-Heisenberg parameter when it (significantly) depended on the spin configuration [28]. However, in this paper, we numerically calculate the implicit configuration dependence of the parameters that are needed to determine the pairwise energy variation $\delta E_{ij}^{\text{two}}$. It should also be noted that it is possible to do a spin-cluster expansion for a description in terms of spin models [29].

This paper is structured as follows. In Sec. II, we will outline the pairwise energy variation formula derived in Ref. [17] for a general, noncollinear spin arrangement. Then, in Sec. III, we summarize the technical details of the density functional theory (DFT) calculations based on the multiple-scattering formalism (MSF) [30]. In Sec. IV, we apply the noncollinear formalism to the system of single-spin rotation. The numerical results are also presented in Sec. IV, while Sec. V summarizes the main conclusions.

II. THEORETICAL BACKGROUND

The fundamental equation of a scalar relativistic MSF is given as [30]

$$\left(\tau_{ij}^{-1}\right)_{L\sigma,L'\sigma'} = p_{iL\sigma\sigma'}\delta_{ij}\delta_{LL'} - G^0_{ij,LL'}\delta_{\sigma\sigma'}, \tag{2}$$

where τ_{ij} stands for the scattering path operator (SPO) and $\mathbf{p}_i = \mathbf{t}_i^{-1}$ denotes the inverse of the single-site scattering operator (ISO). In Eq. (2) $L = (l,m)$ stands for the angular momentum and magnetic quantum numbers, σ refers to the spin index, G^0_{ij} is the free (or bare) structure constant, and indices i and j refer to the considered lattice sites. G^0_{ij} is calculated from the Hamiltonian of the free particle; hence, it is spin independent. Later on, we omit the orbital and spin indices, and the boldface notation stands for quantities in both spin and orbital spaces (18×18 matrices in the *spd* basis), while the lack of boldface refers to quantities defined only in the orbital space (9×9 matrices in the *spd* basis). We introduce a general notation for the single-site scattering operator in a noncollinear framework as

$$\mathbf{t}_i = t_i^0 I_2 + t_i \vec{e}_i \cdot \vec{\sigma}, \tag{3}$$

where the unit vector $\vec{e}_i$ refers to the magnetic spin moment at site i (as already defined in the Introduction) and can be written as

$$\vec{e}_i = (\sin(\theta_i)\cos(\phi_i), \sin(\theta_i)\sin(\phi_i), \cos(\theta_i)), \tag{4}$$

where θ_i and ϕ_i are the polar and azimuthal angles, respectively. $\vec{\sigma}$ is the vector formed by Pauli matrices, I_2 is the unit matrix in spin space, t_i^0 denotes the nonmagnetic (charge) part, and t_i stands for the magnetic (spin) part of the single-site scattering operator. Note that the single-site scattering operator $\mathbf{t}_i$ depends on the energy ε.

For the ISO, one can introduce the same notation as for $\mathbf{t}_i$ in Eq. (3) as follows:

$$\mathbf{p}_i = p_i^0 I_2 + p_i \vec{e}_i \cdot \vec{\sigma}. \tag{5}$$

Later, we will need to deal with the variation of the ISO under a small rotation that can be written as

$$\delta\mathbf{p}_i = p_i \delta\vec{e}_i \cdot \vec{\sigma}, \tag{6}$$

where $\delta\vec{e}_i$ stands for the deviation of a spin moment after an infinitesimal rotation at site i. Finally, the SPO has the structure

$$\tau_{ij} = T_{ij}^0 I_2 + \vec{T}_{ij} \cdot \vec{\sigma}, \tag{7}$$

where T_{ij}^0 denotes the charge and $\vec{T}_{ij} = (T_{ij}^x, T_{ij}^y, T_{ij}^z)$ stands for the spin part of the SPO. In the collinear limit $\vec{T}_{ij}$ is reduced to $(0,0,T_{ij}^z)$, and the components of SPO in the up- and down-spin channels can be defined as $T_{ij}^{\uparrow} = T_{ij}^0 + T_{ij}^z$ and $T_{ij}^{\downarrow} = T_{ij}^0 - T_{ij}^z$.

So far, we have defined the quantities required to calculate the pairwise total energy variation in a noncollinear framework. This can be obtained as the variation of the integrated density of states times energy [19,31]. Due to the Lloyd formula [31], we can write

$$\delta E_{ij}^{\text{two}} = -\frac{1}{\pi}\int_{-\infty}^{\varepsilon_F} d\varepsilon\, \text{Im}\, Tr_{\sigma L}(\delta\mathbf{p}_i \tau_{ij} \delta\mathbf{p}_j \tau_{ji}), \tag{8}$$

where ε_F stands for the Fermi energy. Inserting Eqs. (6) and (7) into Eq. (8) and introducing the matrix

$$A_{ij}^{\alpha\beta} = \frac{1}{\pi}\int_{-\infty}^{\varepsilon_F} d\varepsilon\, \text{Im}\, Tr_L\left(p_i T_{ij}^{\alpha} p_j T_{ji}^{\beta}\right), \tag{9}$$

where indices α and β run over [32] 0, x, y, or z, we get

$$\delta E_{ij}^{\text{two}} = -2\left(A_{ij}^{00} - \sum_{\mu} A_{ij}^{\mu\mu}\right)\delta\vec{e}_i \cdot \delta\vec{e}_j - 4\sum_{\mu,\nu} A_{ij}^{\mu\nu}\delta e_i^{\mu}\delta e_j^{\nu}, \tag{10}$$

where μ and ν run over x, y, and z. In Eq. (10), we have repeated the derivation of Ref. [17] for the noncollinear pairwise energy variation by introducing the quantities we will need to present our results [33].

III. DETAILS OF THE CALCULATIONS

The calculations were performed with the use of standard DFT techniques by means of the real-space linear muffin-tin-orbital method within the atomic-sphere approximation (RS-LMTO-ASA) [34,35]. We employed the standard local-spin-density approximation (LSDA) for the exchange-correlation energy throughout the study.

First, we calculated self-consistently the electronic structure of a system with 8393 Fe atoms arranged into a bcc lattice structure whose inner (core) part can be considered bulklike. The interatomic distance was set to 2.861 Å, while the Wigner-Seitz radius was set to 1.409 Å. Then we embedded nine Fe impurity atoms (one atom and its nearest neighbors) into the Fe bulk host, making it possible to change the direction of the atomistic spins on those atoms and to calculate the electronic structure self-consistently for every θ_i angle which was set at site i while the spin direction on other atoms was kept collinear and ferromagnetic [36]. Note that constraints are neglected in our calculations. Numerical proofs showed, however, that the input angle and the output angle typically varied within 10°.

IV. RESULTS

From a Heisenberg spin model such as the one introduced in Eq. (1), one gets for the pairwise energy variation, in general, that

$$\delta E_{ij}^{\text{two}-H} = -2J_{ij}\delta\vec{e}_i \cdot \delta\vec{e}_j, \tag{11}$$

which is reduced to

$$\delta E_{ij}^{\text{two}-H} = 2J_{ij}\delta\theta_i\delta\theta_j \tag{12}$$

in the collinear limit when only the leading term is kept by inserting the spin variations $\delta\vec{e}_i = (\delta\theta_i,0,0)$ and $\delta\vec{e}_j = (-\delta\theta_j,0,0)$. The symbol H in the expression $\delta E_{ij}^{\text{two}-H}$ refers to the fact that it is derived from the Heisenberg model (1). In this case every spin points to the z direction in a global coordinate system, and a spin at site i and another one at site j are rotated by angles $\delta\theta_i$ and $\delta\theta_j$, respectively. It was shown in Ref. [17] that in this collinear case $J_{ij} = A_{ij}^{00} - A_{ij}^{zz} = A_{ij}^{\uparrow\downarrow}$. The LKAG formula [13] can be derived in the collinear limit where $T_{ij}^{\uparrow}$ and $T_{ij}^{\downarrow}$ can be defined, as shown in Sec. II.

Next, we consider the case when $\vec{e}_i = (\sin\theta_i,0,\cos\theta_i)$, i.e., the spin at site i is rotated in the xz plane by θ_i (see Fig. 1), while every other spin forms a ferromagnetic background, i.e., $\vec{e}_j = (0,0,1)$. This provides a new reference frame for the infinitesimal rotations and will be referred to as the *single-spin rotation*. It can then be shown that $\delta\vec{e}_i = (\cos\theta_i,0,-\sin\theta_i)\delta\theta_i$ when the spin at site i is rotated now by $\delta\theta_i$ while $\delta\vec{e}_j$ remains $(-\delta\theta_j,0,0)$. Inserting $\delta\vec{e}_i$ and $\delta\vec{e}_j$ into Eq. (11), we get for the pairwise energy variation in terms of a Heisenberg model that

$$\delta E_{ij}^{\text{two}-H} = 2J_{ij}\cos(\theta_i)\delta\theta_i\delta\theta_j; \tag{13}$$

that is, we get that the pairwise energy is proportional to $\cos(\theta_i)$, which recovers Eq. (12) in the LKAG limit. Inserting $\delta\vec{e}_i$ and $\delta\vec{e}_j$, however, into Eq. (10), we get for the pairwise energy variation in terms of MSF that

$$\delta E_{ij}^{\text{two}} = 2\left[J_{ij}^{H}\cos(\theta_i) + J_{ij}^{NH}\sin(\theta_i)\right]\delta\theta_i\delta\theta_j, \tag{14}$$

where

$$J_{ij}^{H} = A_{ij}^{00} + A_{ij}^{xx} - A_{ij}^{zz} \tag{15}$$

and

$$J_{ij}^{NH} = -2A_{ij}^{zx}, \tag{16}$$

where the terms which are proportional to $\cos(\theta_i)$ and $\sin(\theta_i)$ are referred to as the Heisenberg (H) term and the non-Heisenberg (NH) term, respectively. It should be stressed that both the Heisenberg, $J_{ij}^{H}(\theta_i)$, and the non-Heisenberg, $J_{ij}^{NH}(\theta_i)$, parameters can implicitly depend on the angle θ_i, too. In the case when $\theta_i = \pi/2$, i.e., when the Heisenberg contribution is zero because $\cos(\pi/2) = 0$, J_{ij}^{NH} can still be finite. In this case the system is *essentially* non-Heisenberg. Otherwise, one should describe it as a Heisenberg model with a configuration-dependent J_{ij}^{H}.

It is easy to show in a collinear case that $J_{ij}^{H} = A_{ij}^{00} - A_{ij}^{zz} = A_{ij}^{\uparrow\downarrow}$; that is, the LKAG formula can be recovered because A_{ij}^{xx} and A_{ij}^{zx} in Eqs. (15) and (16) vanish. Note that we can write as a better approximation that $\delta\vec{e}_i \simeq (\delta\theta_i,0,-1/2(\delta\theta_i)^2)$ and a similar expression for $\delta\vec{e}_j$. Inserting those expressions into Eq. (10), we recover the results for $\delta E_{ij}^{\text{two}}$ published in Ref. [24], where the anisotropic-type term was mapped onto a four-spin Hamiltonian. Note that Eq. (8) should then also be extended with further terms to be correct at the level of the fourth-order approximation in $\delta\theta$. As was reported in Ref. [17], for the nearest-neighbor pairs [37] $A_1^{00} = -0.23$ mRy, while $A_1^{zz} = -1.08$ mRy. This means that the spin contribution (zz) dominates the charge one (00) in the LKAG $J_1 = A_1^{\uparrow\downarrow}$ in bcc Fe, which is given as $A_1^{\uparrow\downarrow} = 0.85$ mRy.

Like for Eq. (1) in Ref. [2], we can decompose the parameters in terms of cubic symmetry-group representations as follows:

$$A_{ij}^{\alpha\beta} = A_{ij}^{\alpha\beta-E_g} + A_{ij}^{\alpha\beta-T_{2g}} + A_{ij}^{\alpha\beta-\text{mix}}, \tag{17}$$

where, as shown in Ref. [38], in some cases, such as for the second-neighbor pairs, the decomposition is complete; however, in general we have a finite mixed term, $A_i^{\alpha\beta-\text{mix}}$. Note that in three-dimensional materials the crystal-field splitting dominates the spin-orbit-coupling interaction; hence, the E-T_{2g} decoupling is meaningful. For the first neighbors we find that $A_1^{\uparrow\downarrow-E_g} = 0.56$ mRy, $A_1^{\uparrow\downarrow-T_{2g}} = -0.99$ mRy, and $A_1^{\uparrow\downarrow-\text{mix}} = 1.29$ mRy. This means that there is a pronounced antiferromagnetic coupling coming from the T_{2g} orbitals (T_{2g} channel) that was shown to be related to Fermi-surface mechanisms (like Ruderman-Kittel-Kasuya-Yosida oscillations calculated in the asymptotic regime) by calculating the exchange parameters for farther neighbor pairs in a given direction. However, in the E_g and mixed channels the microscopic origin is mainly the double-exchange mechanism [2], which requires the presence of the (ferromagnetic) host. Note that we calculate

$A_{ij}^{\alpha\beta}$ in Eq. (9) only for the d electrons. The contributions of the s and p channels are negligible, and the decomposition in Eq. (17) then becomes exact.

As we can see in Eq. (10), the A_{ij}^{00} term contributes only to the Heisenberg-type term, being proportional to $\delta\vec{e}_i \cdot \delta\vec{e}_j$. First, even in the collinear limit we found that $A_1^{00-T_{2g}} = -0.53$ mRy, $A_1^{00-E_g} = 0.12$ mRy, and $A_1^{zz-T_{2g}} = 0.46$ mRy, compared to the larger E_g and mixed contributions, -0.45 and -1.1 mRy, respectively. The source of the anisotropic term (which was reported already in Ref. [24]) is induced by the spin-polarized host due to the double-exchange mechanism. Note that in a paramagnetic phase the $A_{ij}^{\mu\mu}$ terms ($\mu = x,y,z$) are the same in a statistical sense; that is, we cannot speak of terms that are induced by the symmetry-broken host [17]. Host-induced terms are related to the ferromagnetic magnetic order. This mechanism is in analogy to the RKKY interaction: due to scattering mechanisms and based on a s-d interaction model, it can be assumed that the electron spin aligns with the localized magnetic moment orientations. Since our system is close to a ferromagnetic collinear state, electron spins will orientate accordingly. However, scattering of these electrons of a magnetic moment at the single spin rotated by θ_i will transfer angular momentum from the electron to this magnetic moment, which can effectively be considered an extra term in the classical interaction. We refer to these terms as "host-induced" terms. Their role can be crucial and should be analyzed in finite-temperature studies, well above the ordering temperature, when the ferromagnetic background is vanishing, along with their contribution to the Dzyaloshinskii-Moriya interaction, which appears when the spin-orbit interaction is present and the inversion symmetry between the spins is lacking in the system.

We now show that the role of the host-induced terms is more significant for the case of a *single-spin rotation of a noncollinear system* (see Fig. 2). In Fig. 2 the black line shows the relationship between the noncollinear Heisenberg and non-Heisenberg interatomic exchange coupling constants [see Eqs. (15) and (16)] for a nearest-neighbor pair in bcc Fe. The parameters were calculated self-consistently for different θ_i angles (see dots) starting from the collinear ferromagnetic case where $J_1^H = 0.85$ mRy when θ_i was zero, marked by the bigger black symbol. Note that in the final state $\theta_i = \pi$, which is a collinear state. In this case $J_1^{NH} = 0$ and J_1^H can be calculated in terms of the LKAG formalism. The biggest relative change going from zero to π takes place in the E_g channel (red line); that is, this channel together with the mixed contribution is responsible for the configuration dependence of J_1^H as well as the emergence of J_1^{NH}. However, the J_1^H contribution in the T_{2g} channel (see the data in blue) hardly changes as a function of θ_i. In addition, the J_1^{NH} contribution in T_{2g} remains small compared to that in the other channels. This clearly shows for the T_{2g} subspace that the mapping onto a Heisenberg spin Hamiltonian can be done even in the case when one spin is forced to be rotated by a large angle in a ferromagnetic background.

In Fig. 3, where we show the corresponding plot for second-nearest-neighbor interactions, the obtained parameters are in the same energy range in all symmetry channels. Note that the magnitude of J_2^H and J_2^{NH} is much less than that

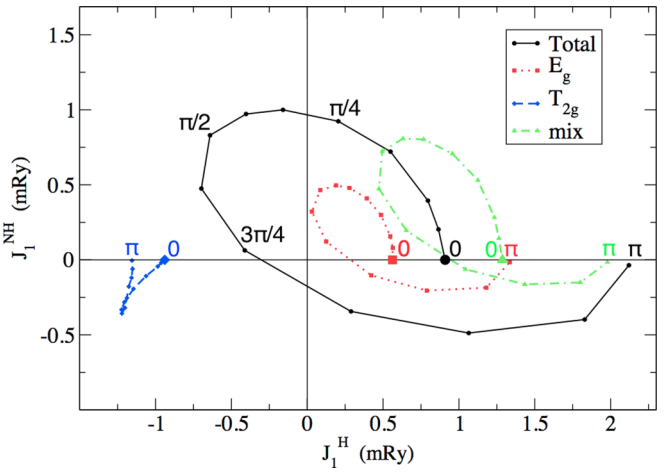

FIG. 2. The black line shows the evolution of the noncollinear interatomic exchange coupling constants for a first-nearest-neighbor pair in bcc Fe single-spin rotation [see Eqs. (15) and (16)]. The red, blue, and green lines show its symmetry decomposition in the d channel defined by Eq. (17). The parameters in the ferromagnetic collinear limit when $\theta_i = 0$ are denoted by bigger symbols. For the nondecomposed (black) curve, $\theta_i = \pi/4$, $\theta_i = \pi/2$, $\theta_i = 3\pi/4$, and $\theta_i = \pi$ are also noted.

of J_1^H and J_1^{NH}. It can be seen in Fig. 4, where the J^H and J^{NH} parameters are shown not only for the first- and second- but also for a third-, fourth-, fifth-, and sixth -neighbor pairs in bcc Fe, that the configuration dependence of the first-neighbor coupling dominates the others. Note that the J^H and J^{NH} parameters are shown as a function of the distance in the Appendix, where the E_g-T_{2g} decomposition of Fig. 4 is also shown in three other figures. In agreement with the previous finding [2,13,17,39], the first- and second-neighbor J_{ij} dominate the J_{ij} calculated for farther neighbors. This conclusion holds in the noncollinear framework too.

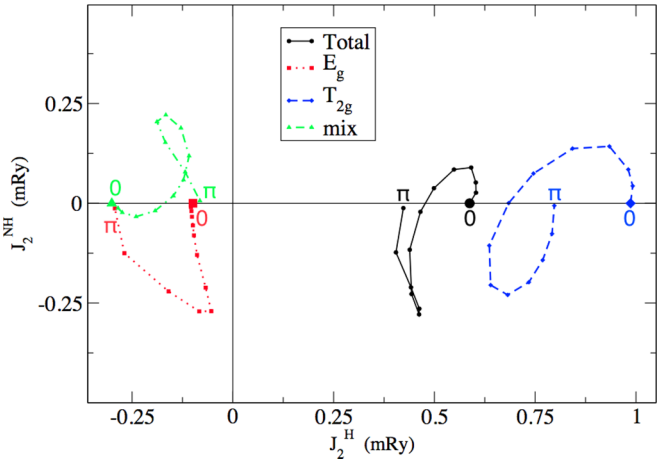

FIG. 3. The black line shows the evolution of the noncollinear interatomic exchange coupling constants for a *second*-nearest-neighbor pair in bcc Fe single-spin rotation [see Eqs. (15) and (16)]. The red, blue, and green lines show its symmetry decomposition in the d channel defined by Eq. (17). The parameters in the ferromagnetic collinear limit when $\theta_i = 0$ are denoted by bigger symbols.

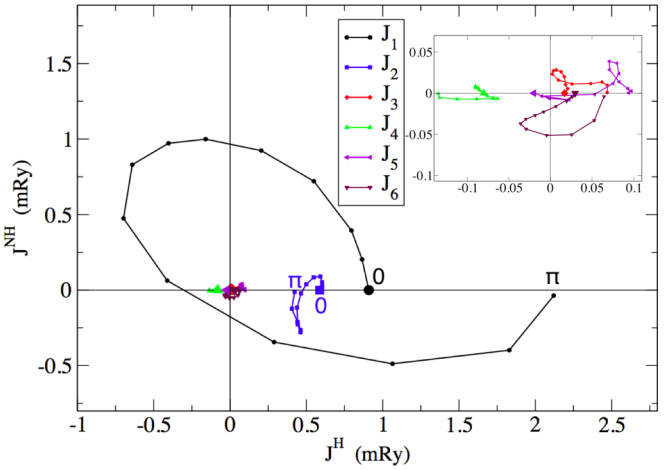

FIG. 4. The calculated J^H and J^{NH} parameters for the first six nearest neighbors in bcc Fe in the (total) d sector in the case of single-spin rotation. The parameters in the ferromagnetic collinear limit when $\theta_i = 0$ are denoted by bigger symbols. Inset: The same parameters for the third, fourth, fifth, and sixth neighbors.

V. CONCLUSIONS

To calculate experimentally detectable quantities such as the critical temperature and the magnon excitation spectra, it is convenient to perform spin dynamics simulations [40] with the description of motion of the atomistic spin. For this purpose the calculation of the interaction parameters between the spins is usually needed.

We have derived for a simple noncollinear spin configuration (when one spin was rotated by a finite angle in a ferromagnetic background) an equation for the energy of the pairwise interaction with terms induced by the spin-polarized host. These terms cannot be completely described by a bilinear Heisenberg spin model. Similar but higher-order host-induced terms were previously found even in the collinear limit also in the absence of spin-orbit coupling when the anisotropic-type terms were mapped onto higher-order (biquadratic) spin Hamiltonians [17,24].

We have shown, however, that an E_g-T_{2g} symmetry analysis based on the decomposition of J_{ij} for the different atomic orbitals in bcc Fe leads to the conclusion that the nearest-neighbor exchange parameters in the T_{2g} channel are *essentially* Heisenberg parameters. This means that they do not depend strongly on the spin configuration *and* can be exactly mapped onto a Heisenberg spin model. These findings are in very good agreement with the conclusions of Ref. [2] based on the LKAG formalism. We also note that the nearest-neighbor angles between the atomistic spins in bcc Fe are usually small at low temperatures (where the background is strongly spin polarized); hence, a Heisenberg model with the LKAG exchange formula can give a good approximation. However, at high temperature, when the angles between the neighboring spins are larger, the background is less polarized.

The role of the host-induced terms and their microscopic origin are crucial (and should be analyzed further) in finite-temperature systems when the ferromagnetic background is vanishing, along with their contribution to the Dzyaloshinskii-Moriya interactions in relativistic calculations. These findings have key importance for strong out-of-equilibrium situations and motivate a general description of an equilibrium case that holds from low temperature (LKAG range) up to the critical temperature (paramagnetic phase). Reference [16] showed that a perturbative expansion to the second order of the Kugel-Khomskii Hamiltonian can be mapped onto a $(J_1 - J_2)$ Heisenberg model. It would be interesting to find whether the Kugel-Khomskii model predicts non-Heisenberg terms for higher-order perturbation theory. The results can also motivate the study of the non-Heisenberg behavior of experimentally realistic systems as ultrafast demagnetization with the use of direct effective-field calculations.

ACKNOWLEDGMENTS

We owe thanks to L. Szunyogh, L. Udvardi, A. Deák, M. Katsnelson, and A. Liechtenstein for fruitful discussions. Support from the Swedish Research Council (VR), the KAW Foundation (Grants No. 2012.0031 and No. 2013.0020), and eSSENCE is acknowledged. The computations were performed on resources provided by the Swedish National Infrastructure for Computing (SNIC). A.B. acknowledges support from CEA-Enhanced Eurotalents, cofunded by the FP7 Marie Skłodowska-Curie COFUND Programme (Grant Agreement No. 600382). P.F.B. acknowledges support from the Icelandic Research Fund (Grant No. 163048-052) and the megagrant of the Ministry of Education and Science of the Russian Federation (Grant No. 14.Y26.31.0015). R.C., D.C.M.R., and A.B.K. acknowledge financial support from Brazilian Federal Agency for Support and Evaluation of Graduate Education (CAPES) and Brazilian National Council for Scientific and Technological Development (CNPq), Brazil.

APPENDIX

In this appendix we present a few additional results of Fig. 4 shown in the main text. Figures 5 and 6 show the Heisenberg and non-Heisenberg parameters for single-spin rotation calculated from the two-site energy variation as a function

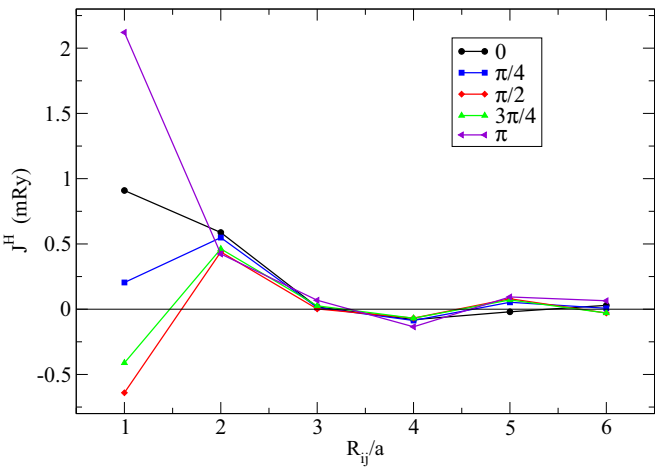

FIG. 5. The calculated Heisenberg parameters for single-spin rotation calculated from the two-site energy variation as a function of distance for four selected angles, $\theta_i = 0, \pi/4, \pi/2, 3\pi/4$, and π.

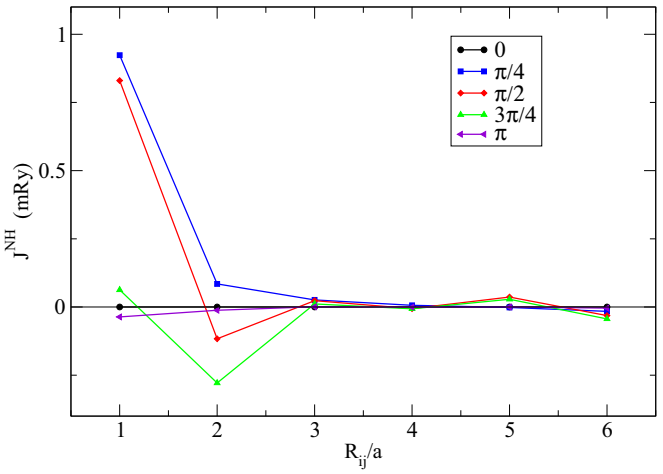

FIG. 6. The calculated non-Heisenberg parameters for single-spin rotation calculated from the two-site energy variation as a function of distance for four selected angles, $\theta_i = 0,\pi/4,\pi/2,3\pi/4$, and π.

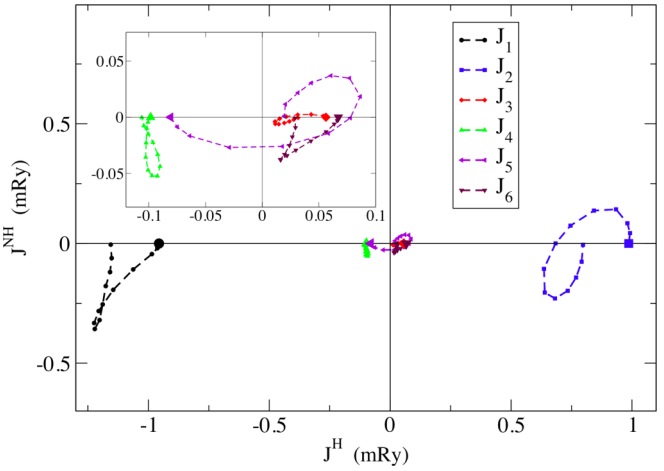

FIG. 8. The calculated J^H and J^{NH} parameters for the first six nearest neighbors in bcc Fe in the T_{2g} sector in the case of single-spin rotation. The parameters in the ferromagnetic collinear limit when $\theta_i = 0$ are denoted by bigger symbols. Inset: The same parameters for the third, fourth, fifth, and sixth neighbors.

of distance for four selected angles, $\theta_i = 0,\pi/4,\pi/2,3\pi/4$, and π. First, we can see that in both cases the strongest configuration dependence is between the nearest-neighbor atoms. Second, the nearest-neighbor Heisenberg parameters shown in Fig. 5 are ferromagnetic for $\theta_i = 0$ and π when the collinear limit is considered and are antiferromagnetic in the extreme noncollinear case ($\theta_i = \pi/2$). The nearest-neighbor Heisenberg parameter has its biggest magnitude in case of $\theta_i = \pi$ due to the strong configuration dependence of the E electrons (see Fig. 2). Third, we note that the non-Heisenberg parameters are zero (up to numerical accuracy) in collinear cases ($\theta_i = 0$ or π).

Finally, Figs. 7, 8, and 9 show the results for the first six nearest neighbors, J^H and J^{NH}, in the E_g, T_{2g}, and mixed-symmetry channels, respectively. In the case of the E_g and the mixed sectors, the configuration dependence of the first-neighbor coupling (denoted by a black line) dominates the others. This can be estimated by comparing the areas that the trajectories span. However, in the T_{2g} case shown in Fig. 8, the configuration dependence of the first- and second-neighbor contributions (black and blue lines) are in the same range. The (absolute) configuration dependence, which is important in the configuration dependence of the spin stiffness, is significantly lower for the farther neighbors in every channel, as shown in the insets in Figs. 7–9.

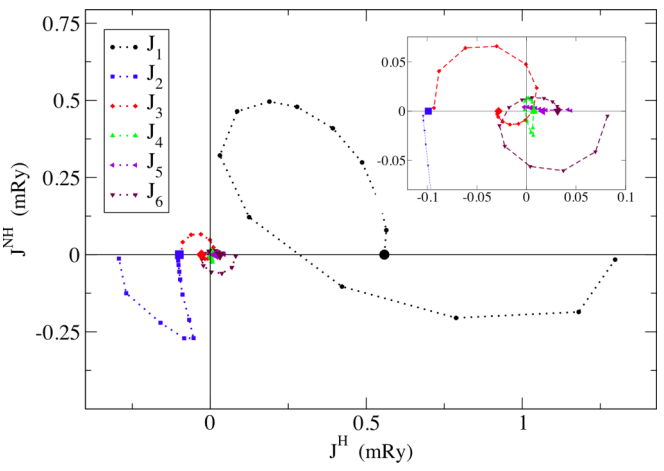

FIG. 7. The calculated J^H and J^{NH} parameters for the first six nearest neighbors in bcc Fe in the E_g sector in the case of single-spin rotation. The parameters in the ferromagnetic collinear limit when $\theta_i = 0$ are denoted by bigger symbols. Inset: The same parameters for the third, fourth, fifth, and sixth neighbors.

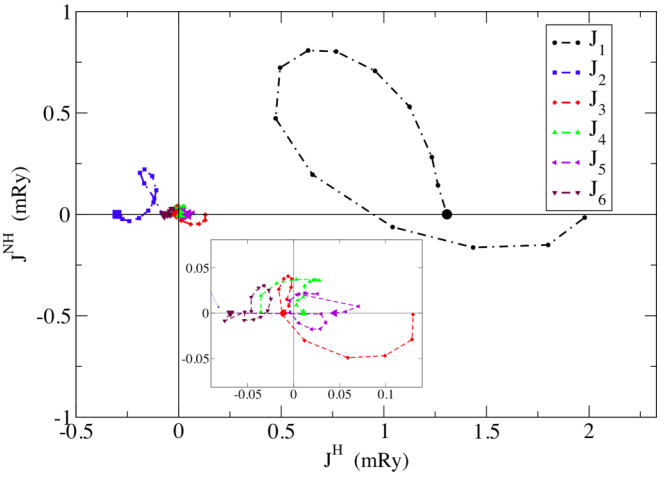

FIG. 9. The calculated J^H and J^{NH} parameters for the first six nearest neighbors in bcc Fe in the mixed sector in the case of single-spin rotation. The parameters in the ferromagnetic collinear limit when $\theta_i = 0$ are denoted by bigger symbols. Inset: The same parameters for the third, fourth, fifth, and sixth neighbors.

[1] P. Fazekas, *Lecture Notes on Electron Correlation and Magnetism* (World Scientific, Singapore, 1999).

[2] Y. O. Kvashnin, R. Cardias, A. Szilva, I. Di Marco, M. I. Katsnelson, A. I. Lichtenstein, L. Nordström, A. B. Klautau, and O. Eriksson, Phys. Rev. Lett **116**, 217202 (2016).

[3] D. Böttcher, A. Ernst, and J. Henk, J. Magn. Magn. Mater. **324**, 610 (2012).

[4] J. Kubler, *Theory of Itinerant Electron Magnetism* (Clarendon, Oxford, 2000).

[5] N. M. Rosengaard and B. Johansson, Phys. Rev. B **55**, 14975 (1997).

[6] P. Mohn, *Magnetism in the Solid State* (Springer, New York, 2003).

[7] S. V. Halilov, H. Eschrig, A. Y. Perlov, and P. M. Oppeneer, Phys. Rev. B **58**, 293 (1998).

[8] V. P. Antropov, B. N. Harmon, and A. N. Smirnov, J. Magn. Magn. Mater. **200**, 148 (1999).

[9] M. I. Katsnelson and A. I. Lichtenstein, Phys. Rev. B **61**, 8906 (2000).

[10] M. Pajda, J. Kudrnovský, I. Turek, V. Drchal, and P. Bruno, Phys. Rev. B **64**, 174402 (2001).

[11] Y. O. Kvashnin, O. Grånäs, I. Di Marco, M. I. Katsnelson, A. I. Lichtenstein, and O. Eriksson, Phys. Rev. B **91**, 125133 (2015).

[12] C. Etz, L. Bergqvist, A. Bergman, A. Taroni, and O. Eriksson, J. Phys. Condens. Matter **27**, 243202 (2015).

[13] A. I. Liechtenstein, M. I. Katsnelson, V. P. Antropov, and V. A. Gubanov, J. Magn. Magn. Mater. **67**, 65 (1987).

[14] L. Udvardi, L. Szunyogh, K. Palotás, and P. Weinberger, Phys. Rev. B **68**, 104436 (2003).

[15] M. I. Katsnelson and A. I. Liechtenstein, J. Phys. Condens. Matter **16**, 7439 (2004).

[16] W. Brzezicki, J. Dziarmaga, and A. M. Oles, Phys. Rev. Lett. **109**, 237201 (2012).

[17] A. Szilva, M. Costa, A. Bergman, L. Szunyogh, L. Nordström, and O. Eriksson, Phys. Rev. Lett. **111**, 127204 (2013).

[18] A. R. Machintosh and O. K. Andersen, in *Electrons at the Fermi Surface*, edited by M. Springford (Cambridge University Press, London, 1980), p. 149.

[19] M. Methfessel and J. Kubler, J. Phys. F **12**, 141 (1982).

[20] R. Lizárraga, L. Nordström, L. Bergqvist, A. Bergman, E. Sjöstedt, P. Mohn, and O. Eriksson, Phys. Rev. Lett. **93**, 127204 (2004).

[21] J. W. Lynn, Phys. Rev. B **11**, 2624 (1975).

[22] D. C. M. Rodrigues, A. Szilva, A. B. Klautau, A. Bergman, O. Eriksson, and C. Etz, Phys. Rev. B **94**, 014413 (2016).

[23] E. Mendive-Tapia and J.e B. Staunton, Phys. Rev. Lett. **118**, 197202 (2017).

[24] S. Lounis and P. H. Dederichs, Phys. Rev. B **82**, 180404(R) (2010).

[25] M. U. Luchini and V. Heine, Europhys. Lett. **14**, 609 (1991).

[26] R. Singer, F. Dietermann, and M. Fähnle, Phys. Rev. Lett. **107**, 017204 (2011).

[27] S. A. Turzhevskii, A. I. Liechtenstein, and M. I. Katsnelson, Fiz. Tverd. Tela **32**, 1952 (1990) [Sov. Phys. Solid State **32**, 1138 (1990)].

[28] Note that not only the rotational dependence of the total energy but also the dependence on the longitudinal fluctuation as well as on the locality of the magnetic moment density should be considered to judge whether a magnetic material is Heisenberg-like.

[29] A. Deák, K. Palotás, L. Szunyogh, and I. A. Szabó, J. Phys. Condens. Matter **27**, 146003 (2015).

[30] B. L. Györffy and G. M. Stocks, in *Electrons in Disordered Metals and Metallic Surfaces*, edited by P. Phariseau, B. L. Györffy, and L. Scheire (Plenum, New York, 1979), p. 193.

[31] P. Lloyd, Proc. Phys. **90**, 207 (1967).

[32] In the collinear LKAG limit α and β run over $\uparrow$ and $\downarrow$, referring to the up- and down-spin channels.

[33] In Sec. II, we refreshed every key step of the derivation of Eq. (10); further details can be found in the Appendix of Ref. [17].

[34] P. R. Peduto, S. Frota-Pessoa, and M. S. Methfessel, Phys. Rev. B **44**, 13283 (1991).

[35] S. Frota-Pessoa, Phys. Rev. B **46**, 14570 (1992).

[36] In this paper we modify the spin direction only for the "center" atom. Also note that the exchange parameters can be calculated for farther-neighbor pairs too.

[37] We use the short notation 1, 2, 3, . . . in the subindex for the nearest, second-nearest, third-nearest, . . . neighboring i-j pairs.

[38] R. Cardias, M. M. Bezerra-Neto, M. S. Ribeiro, A. Bergman, A. Szilva, O. Eriksson, and A. B. Klautau, Phys. Rev. B **93**, 014438 (2016).

[39] S. Frota-Pessoa, R. B. Muniz, and J. Kudrnovsky, Phys. Rev. B **62**, 5293 (2000).

[40] O. Eriksson, A. Bergman, L. Bergqvist, and J. Hellsvik, *Atomistic Spin Dynamics: Foundations and Applications* (Oxford University Press, Oxford, 2017).